Plant Nano Biology 8 (2024) 100075

Contents lists available at ScienceDirect

Plant Nano Biology

journal homepage: www.journals.elsevier.com/plant-nano-biology

Impact of sonication time in nanoparticle synthesis on the nutrition and growth of wheat (*Triticum aestivum* L.) plant☆

Guzin Tombuloglu [a,*], Yassine Slimani [a], Huseyin Tombuloglu [b], Moneerah Alsaeed [b], Emine Akyuz Turumtay [c], Huseyin Sozeri [d], Sultan Akhtar [a], Munirah A. Almessiere [a,e], Halbay Turumtay [f,g,h], Abdulhadi Baykal [i]

[a] Department of Biophysics, Institute for Research and Medical Consultations (IRMC), Imam Abdulrahman Bin Faisal University, P.O. Box 1982, Dammam 31441, Saudi Arabia
[b] Department of Genetics Research, Institute for Research and Medical Consultations (IRMC), Imam Abdulrahman Bin Faisal University, P.O. Box 1982, Dammam 31441, Saudi Arabia
[c] Recep Tayyip Erdogan University, Department of Chemistry, Rize 53020, Turkey
[d] TÜBITAK-UME, National Metrology Institute, P.O. Box 54, Gebze, Kocaeli 41470, Turkey
[e] Department of Physics, College of Science, Imam Abdulrahman Bin Faisal University, P.O. Box 1982, Dammam 31441, Saudi Arabia
[f] Karadeniz Technical University, Department of Energy System Engineering, Trabzon 61830, Turkey
[g] Joint BioEnergy Institute, Emeryville, CA 94608, USA
[h] Environmental Genomics and Systems Biology Division, Lawrence Berkeley National Laboratory, Berkeley, CA 94720, USA
[i] Food Engineering Department, Faculty of Engineering, Istanbul Aydin University, Istanbul 34295, Turkey

ARTICLE INFO

Keywords:
Hard/soft nanocomposites
Elemental analysis
Plant nutrition
Growth
Sonication

ABSTRACT

Nanotechnology in agricultural applications is promising in improving plant nutrition and yield, pest control, and gene delivery. However, the method to synthesize nanoparticles or nanocomposites (NCs) can play a crucial role in determining the characteristics of NCs, such as size and morphology, which may be critical factors affecting plant nutrition and NCs` potential toxicity. This study elucidates the effect of sonication time in synthesizing NCs on its characteristics and plant use efficiency. For this purpose, a hard/soft nanocomposite (NC) ($CoFe_2O_4/Ni_{0.8}Cu_{0.1}Zn_{0.1}Fe_2O_4$) was sonochemically synthesized at different sonication times (20 and 60 minutes) and comprehensively characterized. They were hydroponically applied to wheat seedlings (50, 100, 200, 400, and 800 mg/L). The physiological, morphological, and nutritional status of the seedlings were determined. The results showed that an increase in sonication time decreased the mean NC size: 26.7 nm (20 minutes) and 17.4 nm (60 minutes). Photosynthetic parameters, growth, and biomass were gradually reduced with the increasing NC concentrations, revealing their toxic effect. However, treating NCs at 60 min significantly improved the average root length, suggesting its beneficial role for plant growth at the germination stage. The content of elements in the composition of the NCs (Fe, Zn, Co, Ni, and Cu) was remarkably higher in the NC-treated roots compared to the untreated controls. In addition, 60 minutes of preparation showed better plant uptake than 20 minutes. This is the first study to evaluate the effect of sonication time in the preparation of NC on plant nutrition and their fate in plants.

1. Introduction

Nanoparticles, also known as NPs, are minuscule substances that typically measure between 1 and 100 nanometers in size. They have unique physical and chemical qualities that make them useful in various applications (Ghormade et al., 2011). The potential use of NPs in agriculture, including crop protection, fertilizing, retention of liquid or water, pollution remediation, nanosensors, breeding of plants, and biomolecule delivery, etc., has attracted increasing attention in recent years (Prasad et al., 2017; Kumar et al., 2023). They are also suggested as a fertilizer to help with seed germination, crop protection, and plant growth (Pereira et al., 2019; Mitra et al., 2023). Besides, novel NPs

☆ This article is part of a special issue entitled: "Interactions of Plants with Emerging Nanomaterials and Mixtures" published at the journal Plant Stress.

* Corresponding author.
E-mail address: guzinkekec@gmail.com (G. Tombuloglu).

https://doi.org/10.1016/j.plana.2024.100075
Received 10 March 2024; Received in revised form 23 April 2024; Accepted 6 May 2024
Available online 8 May 2024

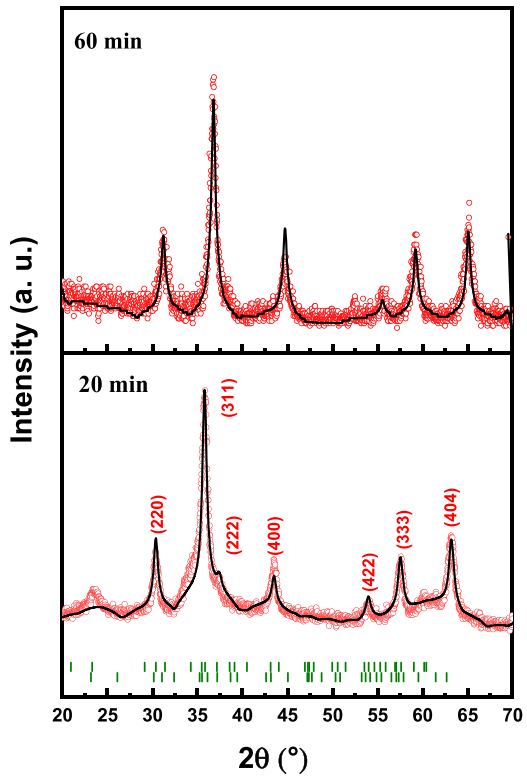

Fig. 1. XRD patterns of hard/soft $CoFe_2O_4/Ni_{0.8}Cu_{0.1}Zn_{0.1}Fe_2O_4$ NCs with different sonication times: 20 (NC20) and 60 (NC60) minutes.

designs can address nutrient deficiency problems in the soil (Agrawal et al., 2022; Yasmine et al., 2023).

Besides their beneficial aspects, NPs can cause toxic effects on living beings. Varied types of NPs behave differently in various environments due to different physicochemical properties responsible for their fate and toxicity (Nowack and Bucheli, 2007; Shin et al., 2015). They can potentially produce genotoxicity, oxidative stress, and growth inhibition in plants (Ranjan et al., 2021). Therefore, the beneficial or toxic effect of each NPs should be investigated before its use on a large scale.

Magnetic nanocomposites (NCs), one of numerous NP kinds, are distinguishable from the others by their magnetic character. They are attractive materials for usage in the biomedical, bioimaging, storing energy, drug delivery, and magnetic semiconductor areas due to their magnetic characteristics (Valan et al., 2015; Hema et al., 2016; Vangijzegem et al., 2019; Nune et al., 2009). Thus far, research on plants associated with the transportation of magnetic NCs has focused on a few types of plants: common beans, pumpkin, tomato, soybean, corn, barley (Zhu et al., 2008; Corredor et al., 2009; Antisari et al., 2013; Ghafariyan et al., 2013; Li et al., 2016; Govea-Alcaide et al., 2016; Tombuloglu et al., 2018, 2019a, 2019b, 2022).

Spinel ferrites are important magnetic materials due to their superior magnetic and electrical characteristics (Abraham, 1994; Amiri et al., 2019; Baykal et al., 2008). Spinel ferrites have a general chemical formula of MFe_2O_4 where M is a divalent metallic ion such as cobalt (Co), nickel (Ni), zinc (Zn), manganese (Mn), copper (Cu), etc. This chemical formula shows that spinel ferrites are magnetic substances made mainly of iron oxide, mixed with other metal elements like Zn, Ni, Mn, etc. It is worth noting that magnetic ferrites are usually categorized as either hard ferrites or soft ferrites. Soft magnetic ferrites display small coercivity, which means they can be magnetized and demagnetized easily by applying a low magnetic field. Hence, they can rapidly and easily change their magnetic orientations and are frequently employed in electrical applications. On the other hand, hard magnetic ferrites display a very large coercivity, which means that they are less susceptible to demagnetization than soft magnetic ferrites. They require the application of an extremely high magnetic field to be demagnetized. Some of the applications of hard spinel ferrites are hard magnets, magnetic recording media, electric motors, stereo speakers, medical diagnostics, etc. One of the methods to determine the magnetic strength of spinel ferrites is the measurements of magnetization versus an applied magnetic field (Figure S1). Combining hard and soft magnetic ferrites can enhance the magnetic features due to the great exchange coupling of both phases. As a consequence, when there is a strong exchange coupling between the soft and hard magnetic phases, the very large coercivity of the hard magnetic phase and the elevated saturation magnetization of the soft magnetic phase will induce an enhancement of different magnetic parameters (large coercivity, high magnetization, strong maximum energy product, etc.) rather than soft and hard phase alone—these outstanding characteristics candidate them for numerous potential applications as permanent magnets.

Several research groups have recently conveyed great efforts to the soft and hard ferrite nanocomposites, primarily for technological (electrical, magnetic, energy, etc.) and medical applications. In the present study, we want to focus on applying hard/soft magnetic ferrite nanocomposites in agriculture/environmental fields. For instance, Khasim et al. (2023) fabricated graphitic carbon nitride (GCN or g-C_3N_4) NCs using Cu/Fe mixed metal oxides for biosensor applications in agriculture. Slimani et al. (2022) synthesized Co, Ni, Cu, Fe, and Zn containing hard/soft NCs, and elucidated the influence of different sonication times on NC characteristics; however, the study does not test NCs` effect on agricultural application. In addition, the development of magnetic spinel ferrite NCs based on cobalt (Co), nickel (Ni), and zinc (Zn) is now underway (Almessiere et al., 2019; Amiri et al., 2019). Spinel ferrite NCs' potential for widespread practical application must be assessed. NCs' synthesis techniques can generally be categorized into three categories: Physical methods, chemical methods, and bio-assisted approaches (Saratale et al., 2018). Sonication is one of the best methods for separating big clusters of NCs into smaller ones (Asadi et al., 2019). This study clarifies the effect of sonication time in synthesizing $CoFe_2O_4/Ni_{0.8}Cu_{0.1}Zn_{0.1}Fe_2O_4$ NCs (NC20 and NC60) by the sonication precipitation technique. After characterization, the NCs were applied to wheat plants, and physiological and morphological changes were assessed. The impact of sonication time on plant nutrition and growth was comprehensively elucidated. This can help researchers choose the optimal sonication time while synthesizing the NCs for agricultural applications.

2. Material and methods

2.1. Synthesis and characterization of nanocomposites

The $CoFe_2O_4/Ni_{0.8}Cu_{0.1}Zn_{0.1}Fe_2O_4$ hard/soft NCs were produced by ultrasonication with varying ultrasonication times: 20 and 60 min (NC20 and NC60, respectively). The $Co(NO_3)_2$, $Ni(NO_3)_2{\cdot}6H_2O$, $Zn(NO_3)_2{\cdot}6H_2O$, $Fe(NO_3)_3.9H_2O$ and $Cu(NO_3)_2{\cdot}6H_2O$ were used as initial materials. The nitrite was mixed in deionized (DI) H_2O (50 mL) at 80 °C (40 min). After that, NaOH was added and dropped wisely until the pH reached 11.5. Ultrasound irradiation (20 kHz and 70 W) was exposed for 20 and 60 min by an ultrasonic homogenizer (UZ SONOPULS HD 2070). To get NCs, the final precursor was repeatedly rinsed with DI water (n = 5) and then dried overnight at 70 °C.

The phase detection of the NCs was performed with an X-ray diffractometer (XRD; D/MAX-2400 (Cu Kα)). A transmission electron microscope (TEM; FEI Titan ST Microscopes) and an energy-dispersive X-ray (EDX) linked to an FE-SEM (Lyra3, Tescan, Brno, Czech Republic) were used to screen the NC morphology. Match 3! software was used to determine the crystallite and structure parameters.

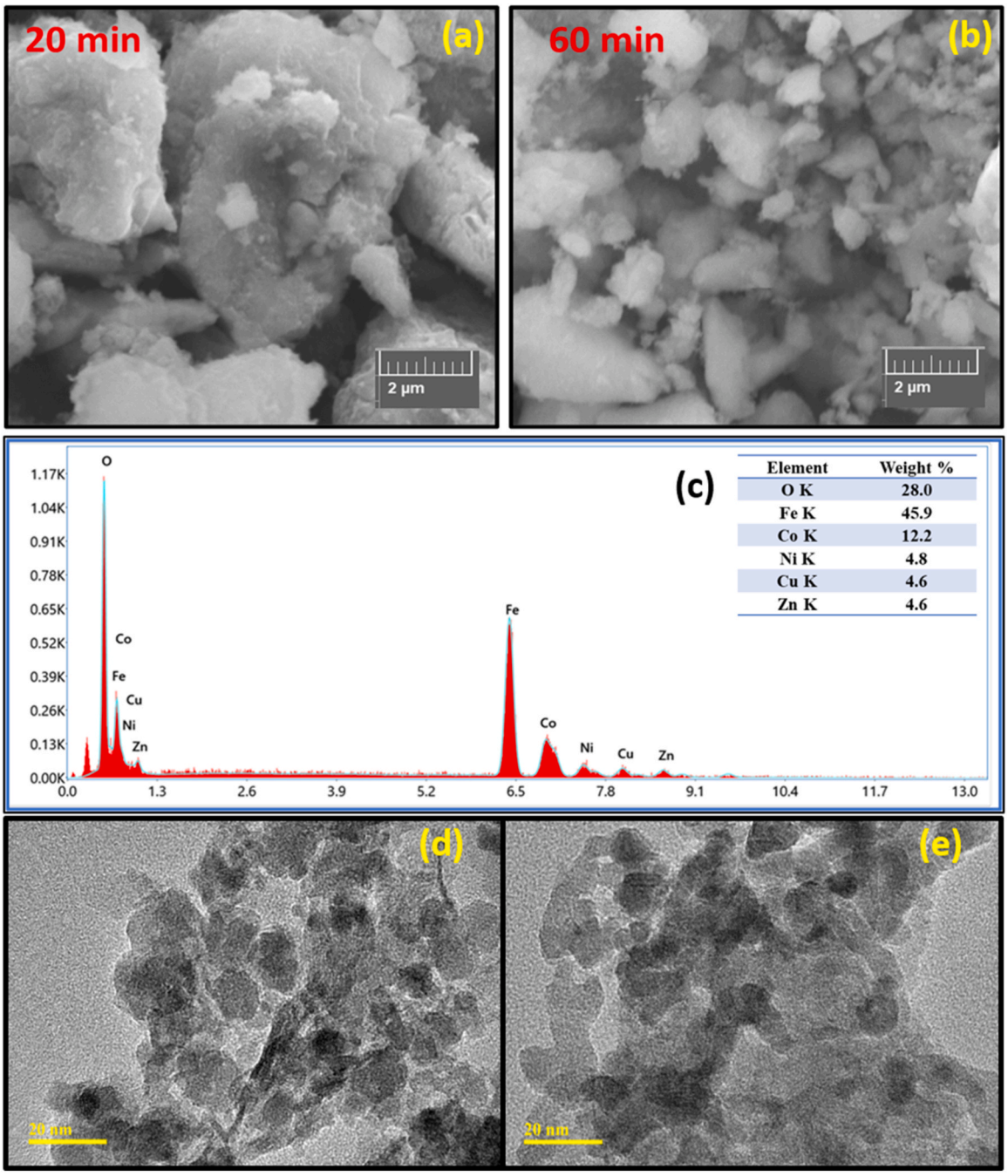

Fig. 2. Characterization of H/S $CoFe_2O_4/Ni_{0.8}Cu_{0.1}Zn_{0.1}Fe_2O_4$ NCs with different sonication times: 20 and 60 minutes (min). (a, b) SEM images, (c) EDX spectrum of NCs. Transmission electron microscopy (TEM) images of (d) NC20 and (e) NC60.

2.2. Nanocomposite treatment and seed/seedling growth

The seeds of wheat (*Triticum aestivum* L.) (n = 20) were planted in Petri plates. The International Seed Testing Association's standard blotting technique was followed to incubate the seeds (Shankramma et al., 2016; ISTA, 2017). NCs in different concentrations (50, 100, 200, 400, and 800 mg/L) were suspended in Hoagland solution: KNO_3 (6 mM), $Ca(NO_3)_2$ (4 mM), $NH_4H_2PO_4$ (1 mM), $MgSO_4$ (2 mM), $CuSO_4$ (0.3 μM), H_3BO_3 (50 μM), $MnCl_2$ (9 μM), $ZnSO_4$ (0.8 μM), Fe-EDTA (0.1 μM), and MoO_3 (85%) (0.12 μM) (Hoagland and Arnon, 1950). The control group was exempt from NC addition. The pH of the solution was kept constant at 6.0 after the preparation of the solution and in the control group. Then, the suspension was applied to wheat seeds and kept for germination for five days in the dark. Before using the seeds, the suspensions were sonicated for thirty minutes in a water bath (Powersonic 410, Hwashin Technology, Korea). A minimum of 0.5 cm of growth was required on 65% of the control roots to declare the seeds germinated (USEPA, 1996). After the germination stage, the seedlings were moved to a hydroponic growth system that was air-pumped supported. The suspension was continuously aerated and changed every three days to provide O_2 demand, better NC dispersion, and avoid agglomeration (Tombuloglu et al., 2023). After three weeks of NC application, the tissues were collected, dried for three days at 70 °C, and broken down to create a fine powder. Dry powder of the plant parts was used for nutrient content and magnetic measurements.

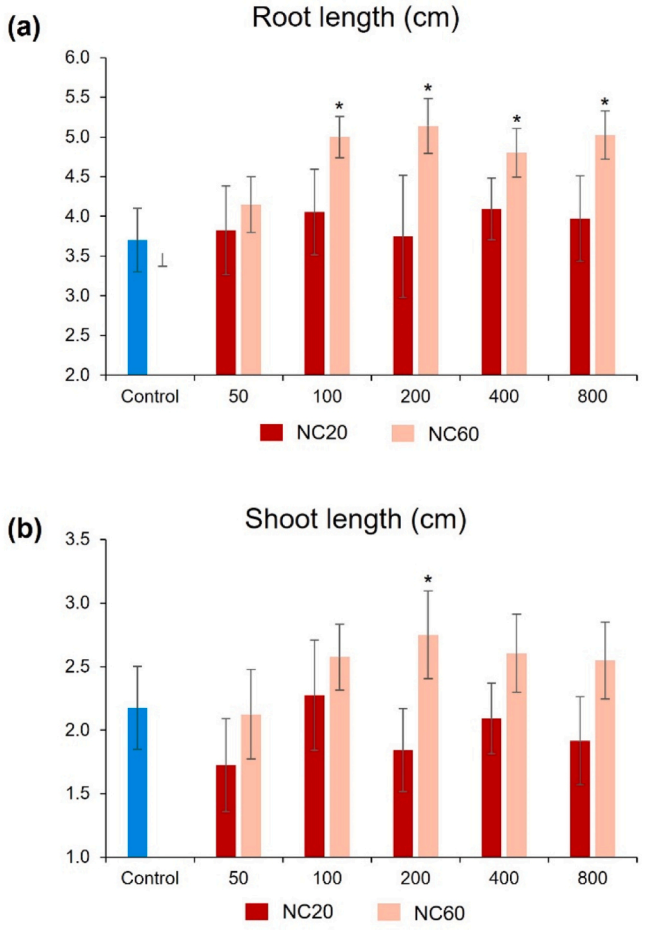

Fig. 3. Root and shoot length of wheat seedlings upon 50–800 mg/L of NC20 and NC60 treatments at the germination stage (five days). (a) Root length, (b) shoot length. Error bars represent +/- standard deviation (SD) (n = 20). * $P < 0.05$.

2.3. Elemental analysis

Dry powder of the plant parts was used for nutrient content and magnetic measurements. Micro- and macro-element concentrations (Fe, Cu, Co, Zn, Mn, Ni, K, Mg, and Ca) were measured in the NC-treated and untreated tissues using a previous protocol (Tombuloglu et al., 2024). The 50 mg of dry tissue was digested (CEM MARSX, CEM) with a mixture (1:4) of nitric acid (HNO_3, 65%) and hydrogen peroxide (H_2O_2, 30%). An inductively coupled plasma optical emission spectrometer (ICP-OES) (PerkinElmer, Scott/Cross-Flow, USA) was used to conduct the elemental analyses following the USEPA method 3051 (USEPA, 2007).

2.4. Scanning electron microscopy (SEM) analysis of roots

The morphology examination of the root was performed using scanning electron microscopy (SEM) (Dart, 1971). Fresh root tips (15 mm) were collected with a sharp blade, rinsed in PBS buffer pH at 7.2, and then preserved in 4% glutaraldehyde for an extended period at 4 °C. Next, a succession of ethanol concentrations of 25%, 50%, 75%, 95%, and 100% were used to dry the tissues. The specimens were gold-coated using rotary pump coating equipment after undergoing critical point drying (Quorum Technologies, Q150R ES, UK) (CPD300, Leica). Then, the specimens were examined under SEM (FEI, Inspect S50, Czech Republic).

2.5. Confocal microscopy observation of roots

The root tips of the plant roots were observed with Propidium iodide (PI) according to a protocol described by Truernit and Haseloff (2008). The PI adheres to living cell walls but cannot pass intact cell membranes. The dye might enter the nucleus through the membrane and stain it since the cell membrane's integrity has been compromised. Therefore, a fluorescence microscope can identify damaged or dead cells. The staining solution dissolved 15 mg of PI (P-4170, Sigma) in 3 mL of dH_2O. The stock solution was then diluted with dH_2O by 1/15 (v/v). The root tips (70 mm) were collected using a razor blade submerged in the 1% PI solution (5 min) to eliminate extra dye particles. The tissues were then rinsed with DI H_2O. The root tips were examined by confocal microscope (LSM 900, Zeiss, Germany) (n = 3). This is how the microscope was set up: the highest emission for PI is 617 nm, the excitation wavelength is 536 nm, and the lasers operate at 488 or 514 nm. The dye only stains intact cells` membranes. However, it penetrates dead cells due to membrane injury and stains the nucleus, which appears red.

2.6. Vibrating sample magnetization (VSM) analysis of plant parts

Magnetic examinations of the plant components were performed to detect any magnetic changes in the plant body after NC treatments. To do this, three weeks-old root and leaf-dried powders from the control and NC-treated groups were analyzed (n = 10). The fine tissue powders were examined with a SQUID-VSM instrument according to the previous study (Tombuloglu et al., 2019b).

2.7. Chlorophyll and carotenoids content

To quantify the pigments (chlorophyll *a*, *b*, and carotenoids), the procedure outlined by Lichtenthaler and Wellburn (1983) was applied. After harvesting, leaf (50 mg) samples were digested with acetone (4 mL, 80%). The homogenate was spun at 4000x g for 15 min, and the absorbances of the supernatant phase were determined (Biotek, Synergy Neo2). To quantify the amounts of carotenoids, chlorophyll *a*, and *b* were carried out using the formula below:

$$\text{Chl-}a = 12.21 \times A_{663} - 2.81 \times A_{646}$$

$$\text{Chl-}b = 20.13 \times A_{646} - 5.03 \times A_{663}$$

$$\text{Car} = (1000 \times A_{470} - 3.27 \times \text{Chl-}a - 104 \times \text{Chl-}b) \div 229$$

2.8. Photosynthetic parameters

The chlorophyll fluorescence in wheat leaves treated with NCs was computed using a fluorometer (Junior-PAM, Walz® GmbH, Effeltrich, Germany). A leaf lip holder was used for the measurements (n = 3). First, the seedlings were kept in a dark room for thirty minutes at room temperature. Then, the photosystem-II photochemical quantum yield (Y (II)), minimum and maximum fluorescence (Fo and Fm), and electron transport rate (ETR) were determined using the WinControl-3.29 software from Walz® GmbH in Effeltrich, Germany (ETR). There was a 150 mmol m^{-2} s^{-1} actinic pulse light employed. Also, the maximum quantum efficiency of PSII (Fv/Fm) and variable fluorescence (Fv) were examined (Kitajima and Butler, 1975).

2.9. Statistical evaluation

The SPSS software (SPSS Inc., Chicago, USA) was used to analyze the data. To compare the samples from the NC-treated and untreated (control) groups, a *t*-test variance analysis was employed. Asterisks were used to denote statistically significant variation (*$P < 0.05$, **$P < 0.01$ and ***$P < 0.005$).

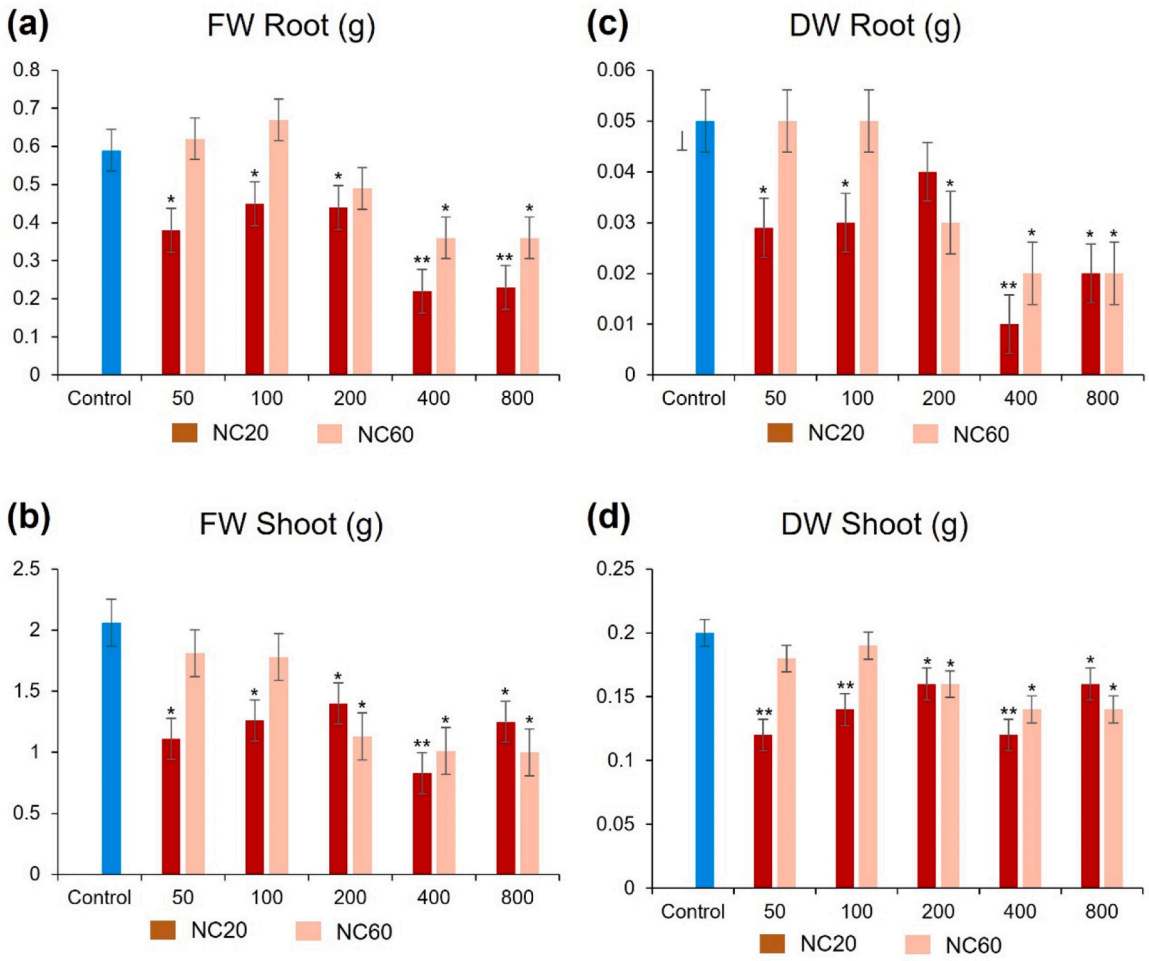

Fig. 4. The fresh weight (FW) and dry weight (DW) of the root and shoot tissues upon 50–800 mg/L of NCs (NC20 and NC60) treatments. (a) Root FW, (b) shoot FW, (c) root DW, and (d) shoot DW. Error bars represent +/- standard deviation (SD) (n = 9). * $P < 0.05$, ** $P < 0.01$.

3. Results

3.1. Effect of sonication time on the structure and morphology of nanocomposites

The XRD pattern of H/S NCs with different sonication times (20 and 60 min) is shown in Fig. 1. The pattern peaks are congruent with the cubic spinel ferrite phase for the mixture of both H/S NCs. Furthermore, the Rietveld analysis of composites agreed on the coexistence of $CoFe_2O_4$ and $Ni_{0.8}Cu_{0.1}Zn_{0.1}Fe_2O_4$. The structure parameters and crystallite were validated by Match 3! Software. The structural parameter "a_o" was 8.2326 and 8.2640 (Å) for 20 and 60 min, while the crystallite size was 26.7 and 17.4 nm, respectively.

The surface analysis of H/S NCs with different sonication times (20 and 60 min) was presented through SEM (Fig. 2a, b). The samples showed chunky grains containing small particles. As the duration of the ultrasonication increased, the size of these particles decreased. The EDX of NCs (60 min) exhibited Co, Fe, Ni, Zn, Cu, and O only (Fig. 2c). The TEM was used to verify the morphology and phase (Figure S2). The TEM results indicated the agglomerate of spherical particles. The HR-TEM is the spinel phase corresponding to XRD results (Figs. 1 and S2).

3.2. Effect of sonication time on germination and plant growth

3.2.1. Growth at the germination stage

Varied NC20 and NC60 concentrations (50, 100, 200, 400, and 800 mg/L) were applied to wheat seeds to understand their effect on germination. While 50 and 100 mg/L doses did not cause a significant change in germination, 200, 400, and 800 mg/L NC applications reduced the germination rate. Compared to NC60, NC20 application caused a more destructive effect on germination at higher concentrations (Figure S3). The average root and shoot length (n = 20) are depicted in Fig. 3. The average root length was significantly improved by the treatment of NC60 ($P < 0.05$), particularly at 200 mg/L treatment. However, the roots or shoots did not alter substantially due to NC20 treatment ($P > 0.05$). This result showed that NC60 is helpful for plant growth at the germination stage, but not NC20. The most beneficial NC60 concentration was 200 mg/L, which increased the root and shoot growth by about 37% and 27%, respectively, compared to the control.

3.2.2. Biomass after three weeks of nanocomposite (NC) treatment

The wheat seedlings were grown with varied concentrations of NC20 and NC60 (50–800 mg/L) for three weeks. Dry weight (DW) and fresh weight (FW) of root and leaf tissues were determined (Fig. 4). Results showed that NC20 significantly diminishes the root and shoot FW starting from 50 mg/L. However, NC60 treatment at 50 and 100 mg/L concentration does not lead to any significant growth suppression. Significant growth retardation was observed at ≥200 mg/L treatments (Figure S4). These results indicated that the sonication time significantly influences plants' growth and biomass. In addition to the concentration, sonication time in the synthesis of NCs influences the toxicity of NCs in wheat seedlings. Therefore, the sonication time in NC synthesis should be considered when implemented in nano-biotechnological applications.

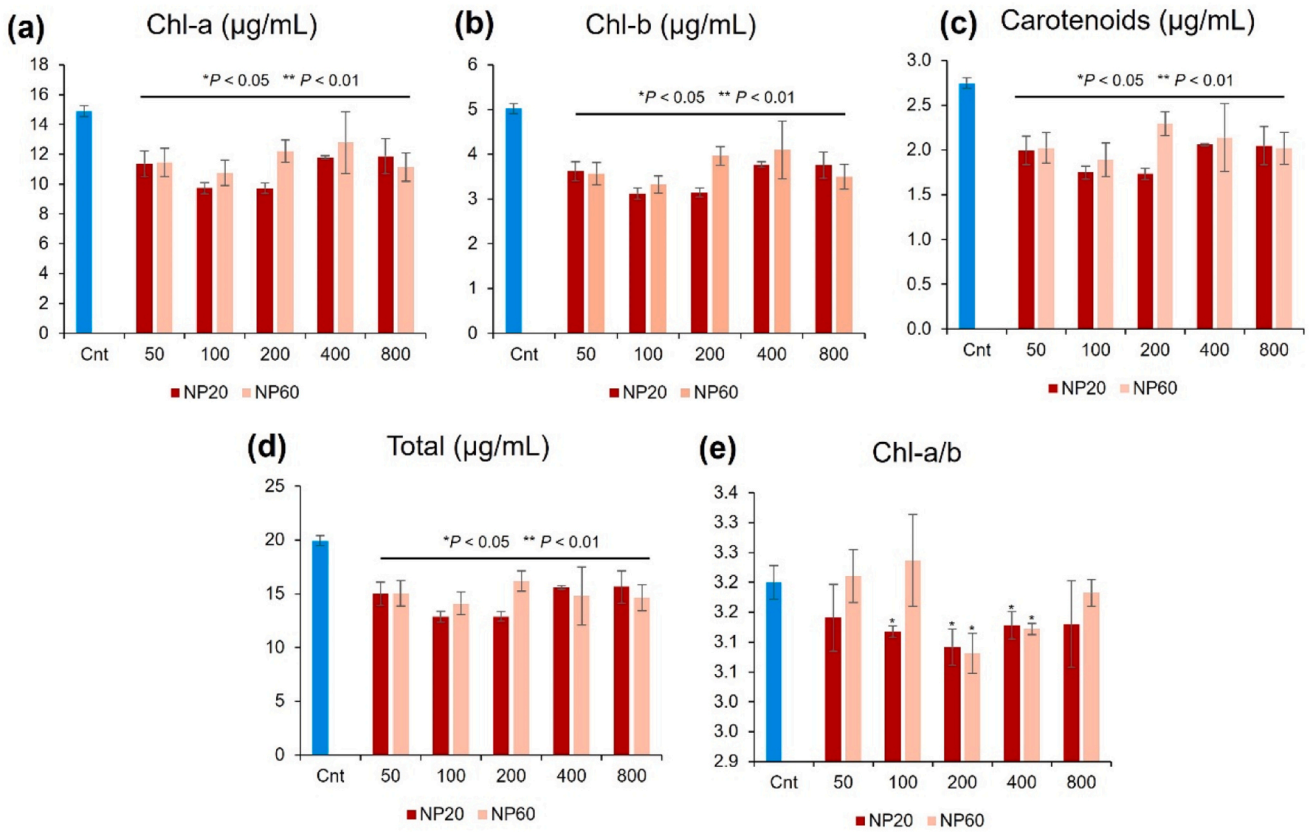

Fig. 5. Effect of different nanocomposite treatments (NC20 and NC60) (50, 100, 200, 400, and 800 mg/L) on pigment (chlorophyll-*a* (Chl-*a*), chlorophyll *b* (Chl-*b*), carotenoids, total chlorophyll, chlorophyll *a* to *b* (Chl-*a*/*b*) ratio) contents (a, b, c, d, e). The Chl-*a*, Chl-*b*, carotenoids, and total chlorophyll units are µg/mL. Cnt denotes the non-treated control plants. The data shows the mean ± SD of biological (n = 8) and technical (n = 3) replicates. * $P < 0.05$, ** $P < 0.01$.

3.3. Pigment and photosynthetic parameters

3.3.1. Chlorophyll and carotenoids content

Fig. 5 depicts that NC20 and NC60 applications decreased the level of pigments such as chlorophyll-*a* (chl-*a*), chlorophyll-*b* (chl-*b*), and carotenoids. Together with these parameters, the Chl-*a* to Chl-*b* ratio (Chl-*a*/*b*), which is one of the most efficient markers representing photosynthetic activity (Racuciu and Creanga, 2007; Ort and Whitmarsh, 2001), was remarkably dropped in all NC applications ($P < 0.05$), except 50 and 100 mg/L of NC60 application (Fig. 6e). This result showed that varied concentrations of NC20 and NC60 treatment diminished the pigmentation of wheat seedlings. However, low concentrations of NC60 (50 and 100 mg/L) are less harmful than NC20.

3.3.2. Photosynthetic parameters

Following NC20 and NC60 treatments at various doses, the chlorophyll fluorescence characteristics (photosystem-II quantum efficiency (Fv/Fm), photosystem-II photochemical quantum yield (Y(II)), and electron transport rate (ETR)) were calculated (Fig. 6). Results showed that Y(II) and ETR significantly dropped upon NC applications ($P < 0.01$). The reduction was gradually increased by increasing the NC concentrations and reached the maximum at 800 mg/L treatment. Compared to the control, the Fv/Fm ratio was increased by the NC60 treatment ($P < 0.05$). This increase was not statistically significant in NC20 applications ($P > 0.05$). The increase in Fv/Fm could be related to the translocation of elements found in the composition of NCs, such as Fe, Zn, Co, Ni, and Cu.

3.4. Uptake and translocation of nanocomposites and plant nutrition

3.4.1. Sonication time affects the nutrition of wheat seedlings

The content of elements found in the composition of NCs (Fe, Zn, Co, Ni, and Cu) were determined in the root and leaf tissues of untreated (control) and NC-treated seedlings. The quantity of elements in the roots was significantly abundant in NC60 compared to the NC20 treatments (Fig. 7). 60-minute preparation (NC60) leads to a faster absorption at lower NC concentration (*i.e.,* 200 mg/L) compared to 20-minute preparation (NC20). The quantities of Fe, Zn, Co, Ni, and Cu were dramatically increased in NCs-treated roots compared to untreated control, verifying the absorption of NCs by roots. In addition, NC treatments altered the macroelement level. For instance, while the level of Mg was found to be decreased, K was noticeably improved compared to the control. In the shoots, the transport of elements found in the NC composition of NCs (Fe, Zn, Co, Ni, and Cu) varied (Fig. 8). For instance, the NC treatments significantly increased the content of Co and Ni in shoots but not Zn, Fe, and Cu. The dramatic increase of Co and Ni in shoots could be attributed to the disassociation of these elements from NCs and their travel to the aerial parts of the plants.

3.4.2. Magnetization analyses

The magnetic properties of plant specimens, precisely specimens from roots and shoots, are investigated to verify these plant parts' uptake of H/S $CoFe_2O_4/Ni_{0.8}Cu_{0.1}Zn_{0.1}Fe_2O_4$ NCs. Fig. 9 shows the magnetization curves against the applied magnetic field, M(H), for root and shoot tissues grown without and with the addition of 800 mg/L of magnetic nanocomposites prepared via sonochemical approach under ultrasonic irradiation durations of 20 and 60 min. As shown in Fig. 9, the degrees of magnetization for different plant tissues are considerably lower than those registered for soft-soft magnetic ferrite nanocomposites

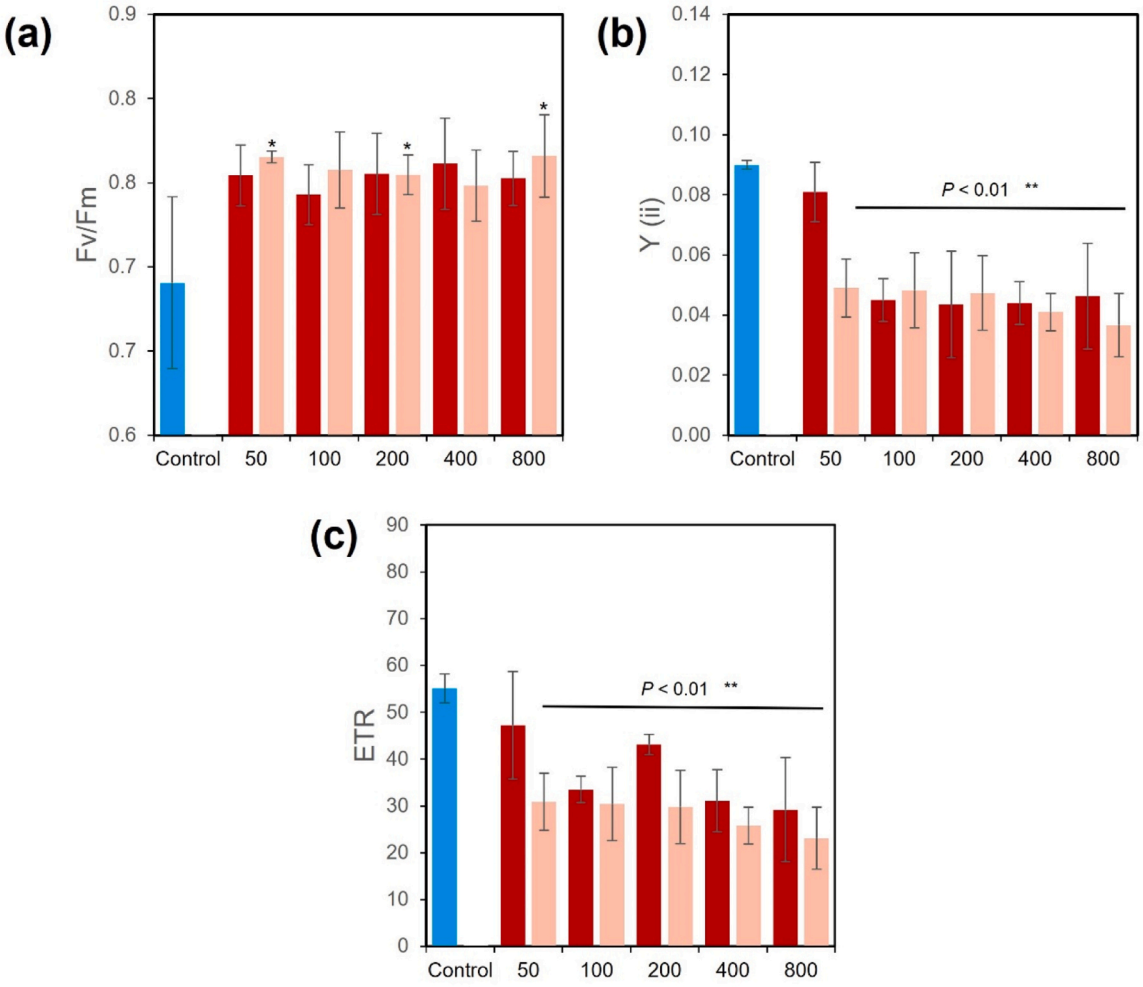

Fig. 6. The photosystem activity indicators (photosystem-II quantum efficiency (Fv/Fm), photosystem-II photochemical quantum yield (Y(II)), and electron transport rate (ETR)) of wheat seedlings upon 50–800 mg/L of NC20 and NC60 applications. (a) Fv/Fm, (b) Y(ii), and (c) ETR. Error bars denote the standard deviation (SD). * $P < 0.05$, ** $P < 0.01$.

(Slimani et al., 2022). This observation is expected to be noticed in stem and shoot specimens. Similar results have been reported in earlier studies by Govea-Alcaide et al. (2016) and Tombuloglu et al. (2019c). The root tissue has grown without the addition of magnetic nanocomposites, as presented in Fig. 9(a), which disclosed the occurrence of ferromagnetic (at lower applied magnetic fields) and diamagnetic (at higher applied magnetic fields) behaviors. Usually, organic plant specimens display diamagnetic behavior in nature (Tombuloglu et al., 2019a, 2019b), and few studies revealed the ferromagnetic behavior of control plant specimens (Tombuloglu et al., 2018). On the other hand, root specimens are grown in an aqueous medium containing 800 mg/L of magnetic nanocomposites prepared via a sonochemical approach under ultrasonic irradiation durations of 20 and 60 min showed a noticeable increment in the magnetization degree compared to the control specimen. The increase in the magnitude of magnetization for these two samples, 800-R-20 and 800-R-60, compared to the control root specimen (CR), suggests the uptake of magnetic nanocomposites by root tissues. Incorporating magnetic nanocomposites within the root tissues will contribute to the final magnetic results and increase the magnetic response. However, one cannot notice any difference between the magnetization results of the control shoot (with the addition of magnetic nanocomposites) and shoot specimens grown in an aqueous medium containing magnetic nanocomposites prepared via sonochemical approach under ultrasonic irradiation durations of 20 and 60 min. Such a finding reflects that the magnetic nanocomposites are not translocated from the roots to the shoot.

This part investigates the impact of the concentration of magnetic NCs. Accordingly, Fig. 10 illustrates the M(H) results of root tissues grown in an aqueous medium containing different concentrations of magnetic NCs (0 mg/L (CR), 200 mg/L (200-R-60), 400 mg/L (400-R-60), and 800 mg/L (800-R-60)) prepared via sonochemical approach under ultrasonic irradiation 60 min. It could be noticed that the magnetization degree increases as the concentration of magnetic NCs increases. The magnetization values at a high applied magnetic field (M_{15} kOe) are shown in Fig. 11. Compared to the control root sample (CR), the M_s value increased to 0.107 emu/g for the 200-R-60 sample, 0.15 emu/g for the 400-R-60 sample, and 0.215 emu/g for the 800-R-60 sample. The intensification of the magnetic signal with the increase in the concentration of magnetic NCs in the aqueous medium for cultivation is ascribed to the uptake of magnetic NCs by the root tissues of the plant (Tombuloglu et al., 2020). This confirms the capability of root tissues to absorb high amounts of the present magnetic NCs. Indeed, the absorption level rises as the magnetic NCs rise within the aqueous medium. Hence, the larger the concentration of magnetic NC uptake is, the greater the magnetization degree will be. Nevertheless, these magnetic NCs are not translocated to the shooting part. A comprehensive mechanism for absorbing magnetic nanomaterials and their nanocomposites is still a challenge to explore.

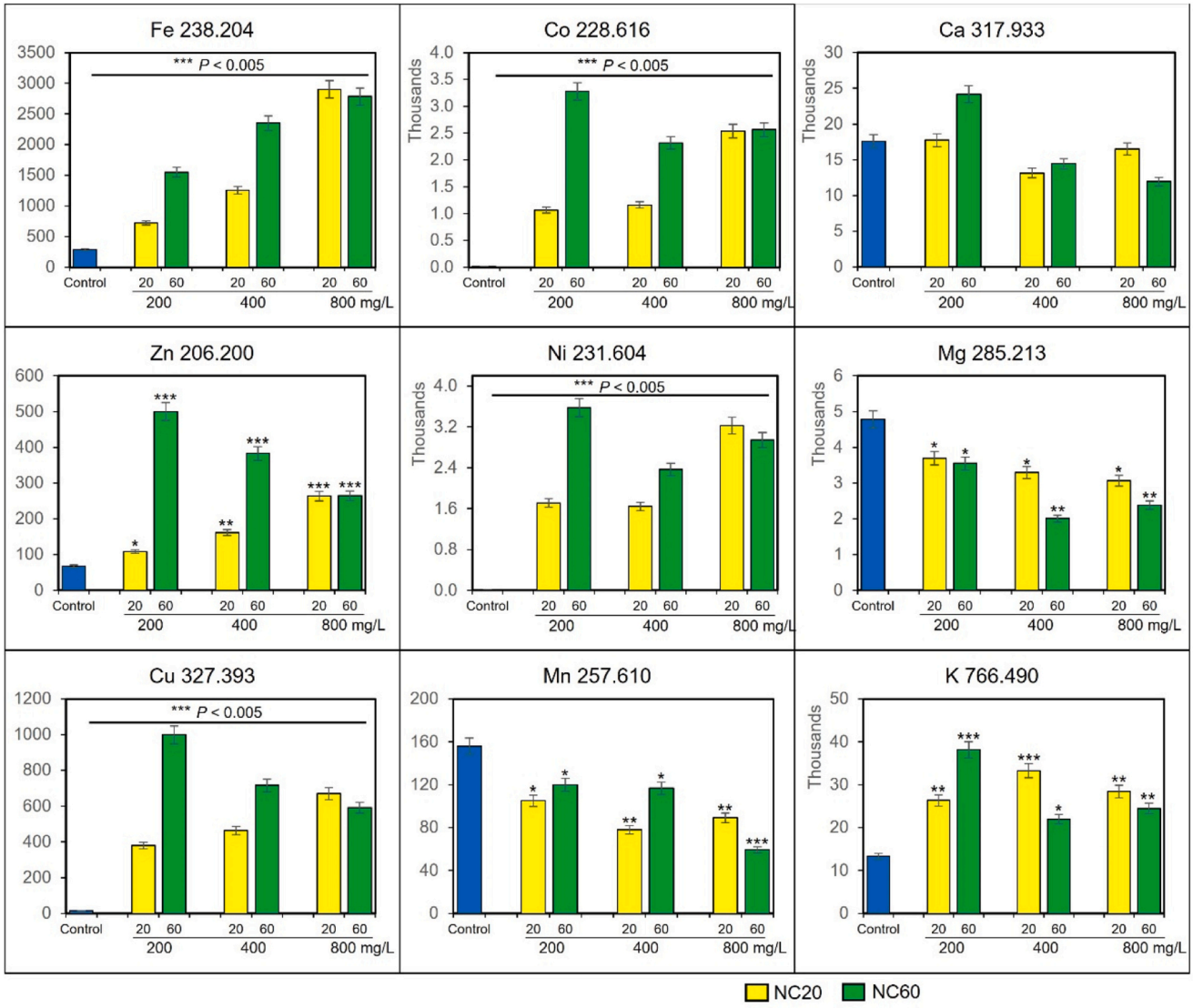

Fig. 7. Elemental analysis of root tissues in control and NC20 and NC60-treated (200, 400, and 800) wheat seedlings. The concentration of nutrient elements (Fe, Zn, Cu, Co, Ni, Mn, Ca, Mg, and K) was represented as mg/kg in dry weight (DW). Each element's absorbance value was indicated on each chart's title. The error bars show three technical replicates' standard deviation (± SD) (n = 3). * $P < 0.05$, ** $P < 0.01$, *** $P < 0.005$.

3.5. Root morphology and cell membrane damage

To evaluate possible morphological damage on root surfaces and possible cell membrane injury by NCs, the roots were examined under an SEM and confocal microscope (Fig. 12). SEM results showed that untreated seedlings have a complete and smooth root surface (Fig. 12a, b). The morphology of the NC-treated samples, however, showed a considerable alteration. Structures began to swell, burst, and shatter at NC concentrations of 400 and 800 mg/L, respectively (Fig. 12c-f). Moreover, NC accumulations on the root surface were apparent. Regardless of the sonication time, NC20 and NC60 caused disruption in root morphology. There was no remarkable difference between the NC20 and NC60 groups (Fig. 12d, f).

The PI dye stains the nucleus in the case of membrane injury. The stained nucleus becomes visible spots under a fluorescence/confocal microscope. Confocal microscopy analysis of the NC-untreated root tips exhibited no cell membrane damage at root tip cells (Fig. 12g). Conversely, the cell membrane injury was evident upon 400 and 800 mg/L treatment (Fig. 12h-j). However, compared to NC20 seedlings, the number of disrupted cells was more prevalent in the NC60-treated seedlings, as shown in Fig. 12i and j, respectively. Overall, SEM and confocal microscopy findings show that NCs at various sonication times (NC20 and NC60) have altered root shape, caused cell membrane injury, and consequently caused root damage. The difference between the NC20 and NC60 applications might be explained by the crystalline size of NCs, where longer sonication times result in smaller particle sizes.

4. Discussion

Herein, the effects of sonication time in the synthesis of hard/soft $CoFe_2O_4/Ni_{0.8}Cu_{0.1}Zn_{0.1}Fe_2O_4$ NCs on the growth and nutrition of wheat (*Triticum aestivum* L.) were investigated. Many chemical and physical applications are used for nanoparticle synthesis, such as irradiation, sonication, pyrolysis, laser ablation, and arc discharge (Jamkhande et al., 2019). Among those, chemical synthesis methods use hazardous reducing agents, producing toxic compounds (Kharissova et al., 2019). Hence, researchers have turned their attention to other methods in their quest for a reliable, secure, nontoxic, and environmentally acceptable way to make NCs. Sonication is one of the best methods for separating big clusters of NCs into smaller ones when synthesizing nanocomposites (Niesz and Morse, 2010). Therefore, this

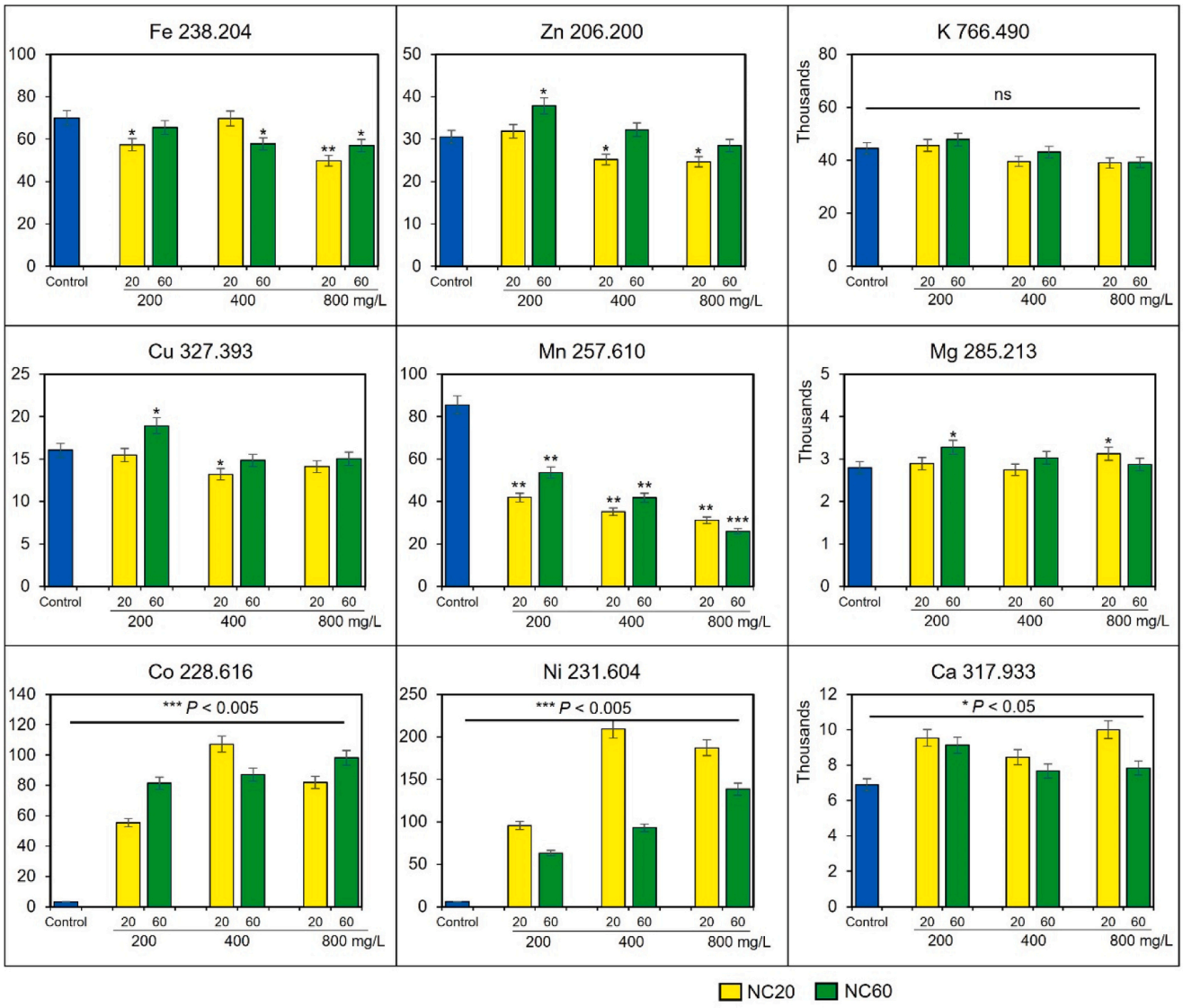

Fig. 8. Elemental analysis of shoot tissues in control and NC20 and NC60-treated (200, 400, and 800) wheat seedlings. The concentration of nutrient elements (Fe, Zn, Cu, Co, Ni, Mn, Ca, Mg, and K) was represented as mg/kg in dry weight (DW). Each element's absorbance value was indicated on each chart's title. The error bars show three technical replicates' standard deviation (± SD) (n = 3, ns = nonsignificant). * $P < 0.05$, ** $P < 0.01$, *** $P < 0.005$.

study used a sonication method. The NCs were sonochemically synthesized with different sonication times: 20 min (NC20) and 60 min (NC60), and then hydroponically applied on plants with a range of concentrations (50–800 mg/L). After the synthesis, the fate and translocation of NC20 and NC60 were assessed by ICP-OES and VSM analyses. The results indicated root uptake of NCs and their migration to the leaves. The inclusion of NCs in the plant tissues results in alterations in nutrient content, plant growth, pigmentation, and photosynthetic parameters (*i.e.,* Fv/Fm, Y(ii), ETR, root, and shoot lengths). The photosynthetic parameters were reduced gradually with NC concentrations (Figs. 5 and 6). Although NCs promote plant growth and development, they can cause toxic effects related to their composition, concentration, and synthesis methods (Ranjan et al., 2021). In line to these results, Shaw and Hossain (2013) reported that Cu NCs reduced seed germination, carotenoid content, root length, and biomass. In addition, a range of hematite (α-Fe_2O_3) NPs (50–400 mg/L) diminished the pigmentation of barley (Tombuloglu et al., 2020). However, the treatment of NC at 60 min significantly improved the average root length (Fig. 3a). This result indicated that NC60 is helpful for plant growth at the germination stage. Compared to the NC20, the NC60 treatment is more useful in growth performance. Moreover, the toxic effects of NCs at high concentrations (200, 400, and 600 mg/L) were obvious at the germination and growth stages (Figures S2, S3). However, higher concentrations of NC60 were less toxic compared to the NC20. This could be attributed to the difference in the size distribution of the NCs. As determined by TEM and HR-TEM, the mean crystallite size of NC20 and NC60 was 26.7 nm and 17.4 nm, respectively (Figure S2). The size distribution is a critical factor that influences the uptake and translocation of NCs in the plant body (Tang et al., 2012; Avellan et al., 2019; Stolte Bezerra Lisboa Oliveira and Ristroph, 2024). In addition, by blocking the membrane pores or disrupting the cellular membranes, they interfere with nutrient trafficking, thus affecting the growth performance of plants (Tombuloglu et al., 2024). The morphological analyses by SEM demonstrated a deformation on the root surfaces (Fig. 12a-f). In addition, confocal microscopy analysis of the root tip cells revealed a membrane injury at higher NC concentrations (Fig. 12g-j). On the other hand, compared to NC20 seedlings, the number of disrupted cells was more prevalent in the NC60-treated seedlings. This could be attributed to the average crystalline size difference between NC20 and NC60. Overall, these findings demonstrate the NC-induced growth inhibition at higher concentrations. The toxic effect could be attributed to the disruption of tissue morphology and cell

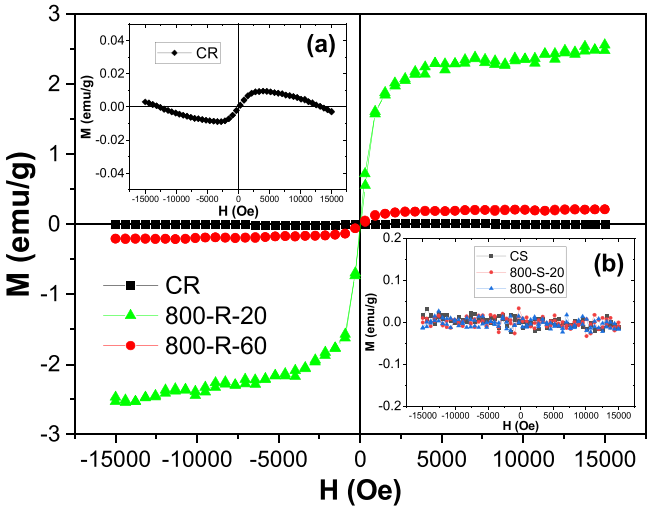

Fig. 9. M(H) curves for root specimens grown without (CR) and with the addition of 800 mg/L of magnetic nanocomposites prepared via sonochemical approach under ultrasonic irradiation durations of 20 and 60 min (800-R-20 and 800-R-60). The inset (a) shows an enlarged view of the M(H) curve of the CR sample. The inset (b) presents M(H) curves for shoot specimens grown without (CS) and with the addition of 800 mg/L of magnetic nanocomposites prepared via sonochemical approach under ultrasonic irradiation durations of 20 and 60 min (800-S-20 and 800-S-60).

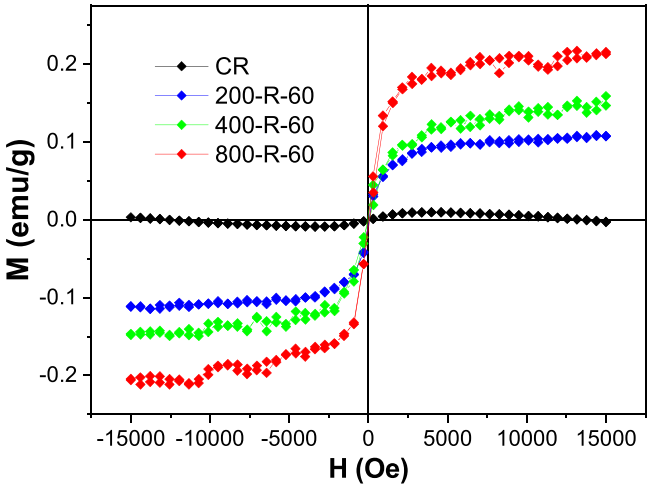

Fig. 10. M(H) results of root tissues grown in an aqueous medium containing different concentrations of NCs ((0 mg/L (CR), 200 mg/L (200-R-60), 400 mg/L (400-R-60), and 800 mg/L (800-R-60)) prepared via sonochemical approach under ultrasonic irradiation 60 min.

membrane injury, which leads to unbalanced nutrient trafficking.

Similarly, the results of dry weight (DW) and fresh weight (FW) of the root and shoot tissues showed that NC20 significantly reduces FW starting from 50 mg/L (Fig. 4). However, the toxic effect of NC20 was observed at >200 mg/L treatments. Al-Amri et al. (2020) indicated that the size of NPs might affect the growth and biomass of the wheat seedlings. In parallel, this study revealed that sonication time influences the NC size (Figure S2). Therefore, obtaining the best NC size for the most efficient plant growth performance should be well considered.

Elemental analysis revealed that NC60 exhibits a better NC absorption at lower concentrations. The content of elements in the composition of the NCs (Fe, Zn, Co, Ni, and Cu) was remarkably abundant in the NC-treated roots compared to the untreated controls (Fig. 7). However, after three weeks of NC application, the quantity of elements increased in

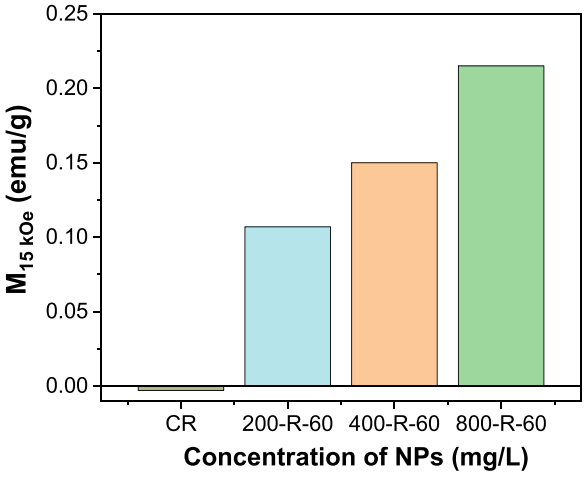

Fig. 11. Magnetization values at the high applied magnetic field (M_{15} kOe) versus the concentration of magnetic nanocomposites within the aqueous medium extracted from VSM data of root specimens.

both the root and shoot tissues (Figs. 7 and 8), but growth did not. On the contrary, the wheat plants' biomass (DW and FW) was decreased compared to the untreated control (Fig. 4). The toxic effects of cobalt ferrites have been shown in different organisms, including mice, humans, zebrafish, and fruit flies (Colognato et al., 2007; Ahmad et al., 2016; Abudayyak et al., 2017; Alaraby et al., 2020). No study is evaluating the effect of sonication time on nanoparticle synthesis in plants. These findings showed that sonication time is a critical factor when preparing NCs, which eventually influences plant nutrient uptake and growth. This study investigated the nutritional status of the wheat plant, the main food source of human beings and the most cultivated crop in the world. Further studies should be performed in the field conditions to understand plant growth performance and nutritional status. Moreover, the potentially toxic effects of NCs should be carefully elucidated to prevent any possible harmful effects on other living beings.

5. Conclusion

In this study, the impact of sonication time on the synthesis of nanocomposite was evaluated by assessing the structural and morphological characteristics and their effect on plant nutrition, physiology, and growth. The results pointed out that sonication time affects the particulate size of the nanocomposites, which eventually impacts the biomineralization and biomass of the wheat plant. The nutritional requirements of each plant are different from each other. Therefore, the nanocomposite should be prepared according to the plant's nutritional needs. In addition to plant-promoting impact, nanocomposites are toxic at higher concentrations and thus should be carefully used. On the other hand, this study shows that the sonication time can be a way to reduce the toxic effect. The less toxic impact of increased sonication time can be attributed to the average size distribution of the nanocomposites. For the first time, this study showed the effect of sonication time during nanocomposite synthesis on plant nutrition and growth. Further studies should consider the time factor and focus on finding the efficient time for the best suitable nanocomposite character according to plant needs.

Ethical approval

This article contains no studies with human participants or animals performed by authors.

Author contributions

GT, MAA, and HT conceptualized the study. YS and HS conducted

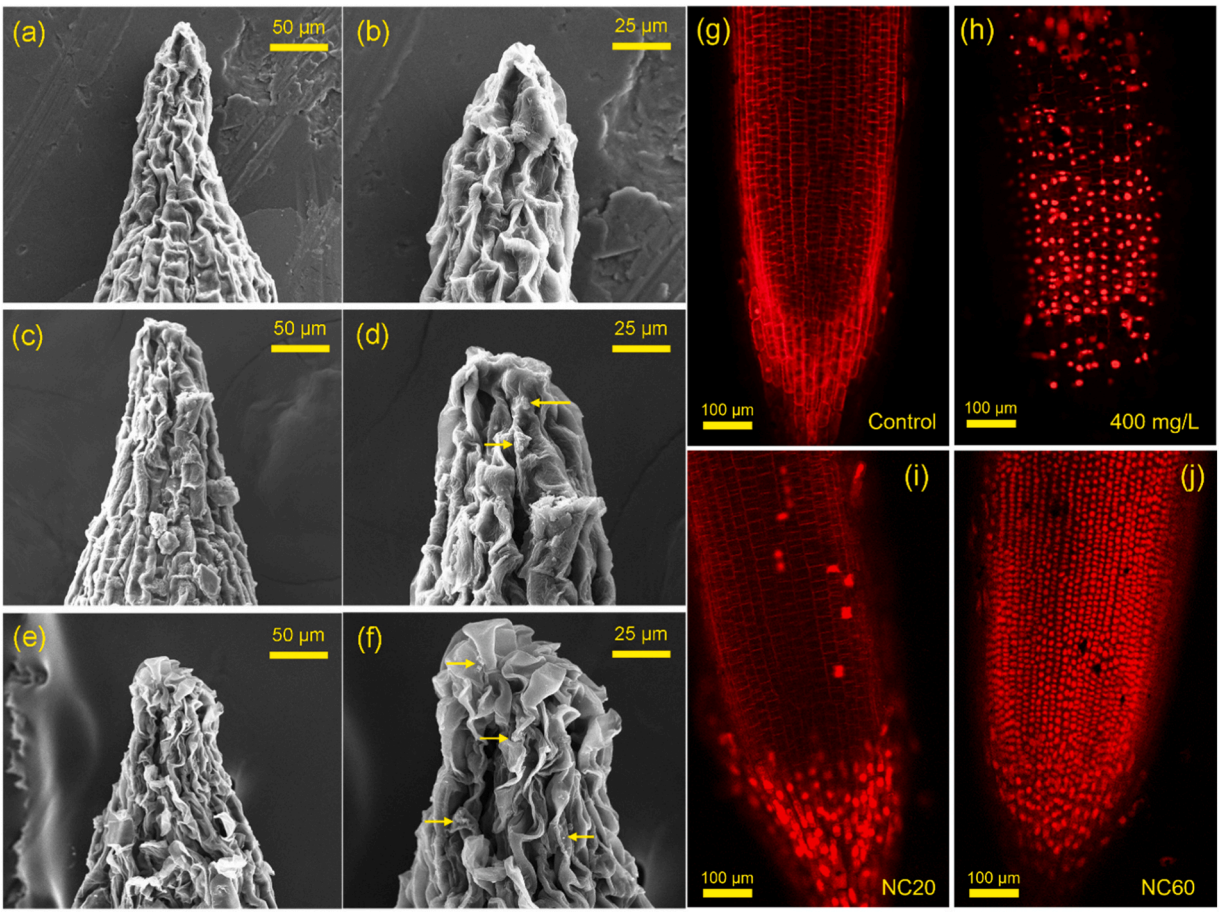

Fig. 12. Scanning electron microscope (SEM) and confocal microscope analyses of root tips grown under different NC concentrations. (a, b) control, (c, d) 400 mg/L, and (e, f) 800 mg/L. Arrows denote NC accumulation sites on the root surface. (g) Control, (h) NC20 of 400 mg/L, (i) NC20 of 800 mg/L, and (j) NC60 of 800 mg/L treatment. The scale bar (a, c, and e) = 50 µm, (b, d, and f) = 25 µm, and (g-h) = 100 µm.

VSM analyses. HT and EAT performed elemental analyses. HT, MA, and GT carried out the physiological experiments. SA conducted TEM and SEM analysis. AB and MAA carried out the nanocomposite synthesis and characterization. GT, HT, YS, MAA, and AB wrote the manuscript. Each author read and approved it.

CRediT authorship contribution statement

Guzin Tombuloglu: Writing – original draft, Methodology, Formal analysis, Data curation, Conceptualization. **Abdulhadi Baykal:** Writing – review & editing, Supervision, Resources. **Halbay Turumtay:** Methodology, Investigation. **Munirah A. Almessiere:** Validation, Supervision, Data curation. **Sultan Akhtar:** Methodology, Investigation. **Huseyin Sozeri:** Methodology, Investigation. **Emine Akyuz Turumtay:** Resources, Methodology, Investigation. **Moneerah Alsaeed:** Methodology, Investigation, Data curation. **Huseyin Tombuloglu:** Writing – original draft, Resources, Project administration, Formal analysis, Data curation, Conceptualization. **Yassine Slimani:** Writing – original draft, Methodology, Investigation, Formal analysis.

Declaration of Competing Interest

The authors declare that they have no known competing financial interests or personal relationships that could have appeared to influence the work reported in this paper.

Data availability

No data was used for the research described in the article.

Acknowledgments

The Deanship of Scientific Research (DSR) fund of Imam Abdulrahman bin Faisal University (IAU) supports the study. Project no: 2019-058-IRMC.

Appendix A. Supporting information

Supplementary data associated with this article can be found in the online version at doi:10.1016/j.plana.2024.100075.

References

Abraham, T., 1994. Nanosized powders of NiZn ferrite: synthesis, structure, and magnetism. Am. Ceram. Soc. Bull. *73*, 62–65.

Abudayyak, M., Altincekic Gurkaynak, T., Özhan, G., 2017. In vitro toxicological assessment of cobalt ferrite nanoparticles in several mammalian cell types. Biol. Trace Elem. Res. *175*, 458–465.

Agrawal, S., Kumar, V., Kumar, S., Shahi, S.K., 2022. Plant development and crop protection using phytonanotechnology: a new window for sustainable agriculture. Chemosphere 299, 134465.

Ahmad, F., Liu, X., Zhou, Y., Yao, H., Zhao, F., Ling, Z., Xu, C., 2016. Assessment of thyroid endocrine system impairment and oxidative stress mediated by cobalt ferrite ($CoFe_2O_4$) nanoparticles in zebrafish larvae. Environ. Toxicol. *31* (12), 2068–2080.

Al-Amri, N., Tombuloglu, H., Slimani, Y., Akhtar, S., et al., 2020. Size effect of iron (III) oxide nanomaterials on the growth, and their uptake and translocation in common wheat (*Triticum aestivum* L.). Ecotoxicol. Environ. Saf. *194*, 110377.

Alaraby, M., Demir, E., Domenech, J., Velázquez, A., Hernández, A., Marcos, R., 2020. In vivo evaluation of the toxic and genotoxic effects of exposure to cobalt nanoparticles using *Drosophila melanogaster*. Environ. Sci. Nano *7* (2), 610–622.

Almessiere, M.A., Slimani, Y., Guner, S., Sertkol, M., Korkmaz, A.D., Shirsath, S.E., Baykal, A., 2019. Sonochemical synthesis and physical properties of $Co_{0.3}Ni_{0.5}Mn_{0.2}Eu_xFe_{2-x}O_4$ nano-spinel ferrites. Ultrason. Sonochem. *58*, 104654.

Amiri, M., Salavati-Niasari, M., Akbari, A., 2019. Magnetic nanocarriers: evolution of spinel ferrites for medical applications. Adv. Colloid Interface Sci. *265*, 29–44.

Antisari, L.V., Carbone, S., Gatti, A., Vianello, G., Nannipieri, P., 2013. Toxicity of metal oxide (CeO_2, Fe_3O_4, SnO_2) engineered nanoparticles on soil microbial biomass and their distribution in soil. Soil Biol. Biochem. *60*, 87–94.

Asadi, A., Pourfattah, F., Szilágyi, I.M., Afrand, M., et al., 2019. Effect of sonication characteristics on stability, thermophysical properties, and heat transfer of nanofluids: a comprehensive review. Ultrason. Sonochem. *58*, 104701.

Avellan, A., Yun, J., Zhang, Y., Spielman-Sun, E., Unrine, J.M., et al., 2019. Nanoparticle size and coating chemistry control foliar uptake pathways, translocation, and leaf-to-rhizosphere transport in wheat. ACS Nano *13* (5), 5291–5305.

Baykal, A., Kasapoğlu, N., Köseoğlu, Y., Toprak, M.S., Bayrakdar, H., 2008. CTAB-assisted hydrothermal synthesis of $NiFe_2O_4$ and its magnetic characterization. J. Alloy. Compd. *464* (1-2), 514–518.

Colognato, R., Bonelli, A., Bonacchi, D., Baldi, G., Migliore, L., 2007. Analysis of cobalt ferrite nanoparticles induced genotoxicity on human peripheral lymphocytes: comparison of size and organic grafting-dependent effects. Nanotoxicology *1* (4), 301–308.

Corredor, E., Testillano, P.S., Coronado, M.J., González-Melendi, P., et al., 2009. Nanoparticle penetration and transport in living pumpkin plants: *in situ* subcellular identification. BMC Plant Biol. *9* (1), 1–11.

Dart, P.J., 1971. Scanning electron microscopy of plant roots. J. Exp. Bot. *22* (1), 163–168.

Ghafariyan, M.H., Malakouti, M.J., Dadpour, M.R., Stroeve, P., Mahmoudi, M., 2013. Effects of magnetite nanoparticles on soybean chlorophyll. Environ. Sci. Technol. *47* (18), 10645–10652.

Ghormade, V., Deshpande, M.V., Paknikar, K.M., 2011. Perspectives for nano-biotechnology enabled protection and nutrition of plants. Biotechnol. Adv. *29* (6), 792–803.

Govea-Alcaide, E., Masunaga, S.H., De Souza, A., Fajardo-Rosabal, L., Effenberger, F.B., Rossi, L.M., Jardim, R.F., 2016. Tracking iron oxide nanoparticles in plant organs using magnetic measurements. J. Nanopart. Res. *18*, 1–13.

Hema, E., Manikandan, A., Gayathri, M., Durka, M., Antony, S.A., Venkatraman, B.R., 2016. The role of Mn^{2+}-doping on structural, morphological, optical, magnetic and catalytic properties of spinel $ZnFe_2O_4$ nanoparticles. J. Nanosci. Nanotechnol. *16* (6), 5929–5943.

Hoagland, D.R., Arnon, D.I., 1950. The water-culture method for growing plants without soil. Circ. Calif. Agric. Exp. Station *347* (2nd edit), 4–32.

ISTA, 2017. International Rules for Seed Testing. International Seed Testing Association, Bassersdorf, Switzerland.

Jamkhande, P.G., Ghule, N.W., Bamer, A.H., Kalaskar, M.G., 2019. Metal nanoparticles synthesis: An overview on methods of preparation, advantages and disadvantages, and applications. J. Drug Deliv. Sci. Technol. 53, 101174.

Kharissova, O.V., Kharisov, B.I., Oliva González, C.M., Méndez, Y.P., López, I., 2019. Greener synthesis of chemical compounds and materials. R. Soc. Open Sci. *6* (11), 191378.

Khasim, S., Pasha, A., Dastager, S.G., Panneerselvam, C., et al., 2023. Design and development of multi-functional graphitic carbon nitride heterostructures embedded with copper and iron oxide nanoparticles as versatile sensing platforms for environmental and agricultural applications. Ceram. Int. *49* (12), 20688–20698.

Kitajima, M.B.W.L., Butler, W.L., 1975. Quenching of chlorophyll fluorescence and primary photochemistry in chloroplasts by dibromothymoquinone. Biochim. Biophys. Acta (BBA) Bioenerg. *376* (1), 105–115.

Kumar, P., Malik, S., Dubey, K.K., 2023. A review on the use of nanomaterials in agriculture: benefits and associated health risks. Curr. Nanomater. *8* (1), 44–57.

Li, J., Hu, J., Ma, C., Wang, Y., Wu, C., et al., 2016. Uptake, translocation and physiological effects of magnetic iron oxide (γ-Fe_2O_3) nanoparticles in corn (*Zea mays* L.). Chemosphere 159, 326–334.

Lichtenthaler, H.K., Wellburn, A.R., 1983. Determinations of total carotenoids and chlorophylls a and b of leaf extracts in different solvents. Biochem. Soc. Trans. 603, 591–592.

Mitra, D., Adhikari, P., Djebaili, R., Thathola, P., Joshi, K., et al., 2023. Biosynthesis and characterization of nanoparticles, its advantages, various aspects and risk assessment to maintain the sustainable agriculture: emerging technology in modern era science. Plant Physiol. Biochem. 196, 103–120.

Niesz, K., Morse, D.E., 2010. Sonication-accelerated catalytic synthesis of oxide nanoparticles. Nano Today *5* (2), 99–105.

Nowack, B., Bucheli, T.D., 2007. Occurrence, behavior and effects of nanoparticles in the environment. Environ. Pollut. *150* (1), 5–22.

Nune, S.K., Gunda, P., Thallapally, P.K., Lin, Y.Y., Laird Forrest, M., Berkland, C.J., 2009. Nanoparticles for biomedical imaging. Expert Opin. Drug Deliv. *6* (11), 1175–1194.

Ort, D., Whitmarsh, J., 2001. Photosynthesis. Encyclopedia of Life Sciences. Macmillan, London.

Pereira, A.D.E.S., Oliveira, H.C., Fraceto, L.F., 2019. Polymeric nanoparticles as an alternative for application of gibberellic acid in sustainable agriculture: a field study. Sci. Rep. *9* (1), 7135.

Prasad, R., Bhattacharyya, A., Nguyen, Q.D., 2017. Nanotechnology in sustainable agriculture: recent developments, challenges, and perspectives. Front. Microbiol. *8*, 1014.

Racuciu, M., Creanga, D., 2007. TMA-OH coated magnetic nanoparticles internalized in vegetal tissue. Rom. J. Phys. *52* (3/4), 395.

Ranjan, A., Rajput, V.D., Minkina, T., Bauer, T., Chauhan, A., Jindal, T., 2021. Nanoparticles induced stress and toxicity in plants. Environ. Nanotechnol. Monit. Manag. *15*, 100457.

Saratale, R.G., Saratale, G.D., Shin, H.S., Jacob, J.M., Pugazhendhi, A., Bhaisare, M., Kumar, G., 2018. New insights on the green synthesis of metallic nanoparticles using plant and waste biomaterials: current knowledge, their agricultural and environmental applications. Environ. Sci. Pollut. Res. *25*, 10164–10183.

Shankramma, K., Yallappa, S., Shivanna, M.B., Manjanna, J., 2016. Fe 2 O 3 magnetic nanoparticles to enhance S. lycopersicum (tomato) plant growth and their biomineralization. Appl. Nanosci. *6*, 983–990.

Shaw, A.K., Hossain, Z., 2013. Impact of nano-CuO stress on rice (*Oryza sativa* L.) seedlings. Chemosphere *93*, 906–915.

Shin, S.W., Song, I.H., Um, S.H., 2015. Role of physicochemical properties in nanoparticle toxicity. Nanomaterials *5* (3), 1351–1365.

Slimani, Y., Almessiere, M.A., Baykal, A., Gondal, M.A., Tashkandi, N., 2022. Impact of sonication time on the structural and magnetic features of $CoFe_2O_4$/$Ni_{0.8}Cu_{0.1}Zn_{0.1}Fe_2O_4$ hard-soft nanocomposites. J. Alloy. Compd. *923*, 166347.

Stolte Bezerra Lisboa Oliveira, L., Ristroph, K.D., 2024. Critical review: uptake and translocation of organic nanodelivery vehicles in plants. Environ. Sci. Technol. *58* (*13*), 5646–5669.

Tang, L., Fan, T.M., Borst, L.B., Cheng, J., 2012. Synthesis and biological response of size-specific, monodisperse drug–silica nanoconjugates. ACS Nano *6* (5), 3954–3966.

Tombuloglu, G., Aldahnem, A., Tombuloglu, H., Slimani, Y., et al., 2024. Uptake and bioaccumulation of iron oxide nanoparticles (Fe_3O_4) in barley (*Hordeum vulgare* L.): effect of particle-size. Environ. Sci. Pollut. Res. *31*, 22171–22186.

Tombuloglu, H., Ercan, I., Alqahtani, N., Alotaibi, B., et al., 2023. Impact of magnetic field on the translocation of iron oxide nanoparticles (Fe_3O_4) in barley seedlings (*Hordeum vulgare* L.). 3 Biotech *13* (9), 296.

Tombuloglu, H., Slimani, Y., Tombuloglu, G., et al., 2019c. Impact of superparamagnetic iron oxide nanoparticles (SPIONs) and ionic iron on physiology of summer squash (*Cucurbita pepo*): a comparative study. Plant Physiol. Biochem. *139*, 56–65.

Tombuloglu, H., Slimani, Y., Tombuloglu, G., et al., 2019b. Tracking of $NiFe_2O_4$ nanoparticles in barley (*Hordeum vulgare* L.) and their impact on plant growth, biomass, pigmentation, catalase activity, and mineral uptake. Environ. Nanotechnol. Monit. Manag. *11*, 100223.

Tombuloglu, H., Slimani, Y., Tombuloglu, G., et al., 2019a. Uptake and translocation of magnetite (Fe_3O_4) nanoparticles and its impact on photosynthetic genes in barley (*Hordeum vulgare* L.). Chemosphere 226, 110–122.

Tombuloglu, H., Slimani, Y., Akhtar, S., Alsaeed, M., et al., 2022. The size of iron oxide nanoparticles determines their translocation and effects on iron and mineral nutrition of pumpkin (*Cucurbita maxima* L.). J. Magn. Magn. Mater. *564*, 170058.

Tombuloglu, H., Slimani, Y., AlShammari, T.M., Bargouti, M., et al., 2020. Uptake, translocation, and physiological effects of hematite (α-Fe_2O_3) nanoparticles in barley (*Hordeum vulgare* L.). Environ. Pollut. *266*, 115391.

Tombuloglu, H., Tombuloglu, G., Slimani, Y., et al., 2018. Impact of manganese ferrite ($MnFe_2O_4$) nanoparticles on growth and magnetic character of barley (*Hordeum vulgare* L.). Environ. Pollut. *243*, 872–881.

Truernit, E., Haseloff, J., 2008. A simple way to identify non-viable cells within living plant tissue using confocal microscopy. Plant Methods *4*, 1–6.

USEPA (United States Environmental Protection Agency), 1996. Ecological Effects Test Guidelines: Seed Germination/root Elongation Toxicity Test. Prevention, Pesticides and Toxic Substances, Washington, DC, 710.

USEPA (United States Environmental Protection Agency), 2007. Method 3051A - Microwave Assisted Acid Digestion of Sediments, Sludges, Soils, and Oils. Revision 1. Washington, DC.

Valan, M.F., Manikandan, A., Antony, S.A., 2015. A novel synthesis and characterization studies of magnetic Co_3O_4 nanoparticles. J. Nanosci. Nanotechnol. *15* (6), 4580–4586.

Vangijzegem, T., Stanicki, D., Laurent, S., 2019. Magnetic iron oxide nanoparticles for drug delivery: applications and characteristics. Expert Opin. Drug Deliv. *16* (1), 69–78.

Yasmine, R., Ahmad, J., Qamar, S., Qureshi, M.I., 2023. Engineered nanomaterials for sustainable agricultural production, soil improvement and stress management. Plant Biology, Sustainability and Climate Change. Elsevier, Amsterdam, The Netherlands, pp. 495–512.

Zhu, H., Han, J., Xiao, J.Q., Jin, Y., 2008. Uptake, translocation, and accumulation of manufactured iron oxide nanoparticles by pumpkin plants. J. Environ. Monit. *10* (6), 713–717.